Biochimica et Biophysica Acta 1842 (2014) 1350–1363

Contents lists available at ScienceDirect

Biochimica et Biophysica Acta

journal homepage: www.elsevier.com/locate/bbadis

Discoidin domain receptor 2 facilitates prostate cancer bone metastasis *via* regulating parathyroid hormone-related protein

Zhang Yan [a], Su Jin [d], Zhang Wei [e], Hou Huilian [b], Yin Zhanhai [c], Teng Yue [a], Li Juan [a], Li Jing [a], Yao Libo [d], Li Xu [a,*]

[a] Center for Translational Medicine, The First Affiliated Hospital of Xi'an Jiaotong University College of Medicine, Xi'an, PR China
[b] Department of Pathology, The First Affiliated Hospital of Xi'an Jiaotong University College of Medicine, Xi'an, PR China
[c] Department of Orthopaedics, The First Affiliated Hospital of Xi'an Jiaotong University College of Medicine, Xi'an, PR China
[d] Department of Biochemistry and Molecular Biology, The Fourth Military Medical University, Xi'an, PR China
[e] Department of Biopharmaceutics, The Fourth Military Medical University, Xi'an, PR China

ARTICLE INFO

Article history:
Received 9 December 2013
Received in revised form 26 March 2014
Accepted 21 April 2014
Available online 27 April 2014

Keywords:
Prostate cancer
Bone metastasis
DDR2
Runx2
PTHrP

ABSTRACT

Prostate cancer frequently metastasizes to the skeleton but the underlying mechanism remains largely undefined. Discoidin domain receptor 2 (DDR2) is a member of receptor tyrosine kinase (RTK) family and is activated by collagen binding. This study aimed to investigate the function and detailed mechanism of DDR2 in prostate cancer bone dissemination. Herein we found that DDR2 was strongly expressed in bone-metastatic prostate cancer cells and tissues compared to that in normal controls. Enhanced expression of constitutively activated DDR2 led to elevation in motility and invasiveness of prostate cancer cells, whereas knockdown of DDR2 through specific shRNA caused a dramatic repression. Knockdown of DDR2 in prostate cancer cells resulted in significant decrease in the proliferation, differentiation and function of osteoblast. Over-expression of DDR2 in prostate cancer cells resulted in notable acceleration of osteoclast differentiation and bone resorption, whereas knockdown of DDR2 exhibited the opposite effects. An intrabone injection bone metastasis animal model demonstrated that DDR2 promoted osteolytic metastasis *in vivo*. Molecular evidence demonstrated that DDR2 regulated the expression, secretion, and promoter activity of parathyroid hormone-related protein (PTHrP), *via* modulating Runx2 phosphorylation and transactivity. DDR2 was responsive to TGF-β and involved in TGF-β-mediated osteoclast activation and bone resorption. In addition, DDR2 facilitated prostate cancer cells adhere to type I collagen. This study reveals for the first time that DDR2 plays an essential role in prostate cancer bone metastasis. The mechanism disclosure may provide therapeutic targets for the treatment of prostate cancer.

1. Introduction

Prostate cancer (PCa) is the second most frequently diagnosed cancer and the second leading cause of cancer death in men after lung cancer [1,2]. The incidence and mortality rate of prostate cancer are significantly higher in developed countries especially the United States, where 186,000 new cases are diagnosed and 28,600 deaths occurred due to it in 2008 [3]. In the United Kingdom, the statistic data was about 35,000 cases and 10,000 deaths annually [4]. The skeleton is the most frequent metastatic site for aggressive prostate cancer, with a frequency of nearly 80%. Prostate cancer bone metastases cause intractable pain, spinal cord compression, pathologic fracture, hypercalcemia, and lead to poor quality of life as well as reduced life expectancy [5].

The progression of prostate cancer metastasizing to the bones is a complex process involving bone-tumor cell crosstalk mediated by various cytokines and factors [6,7]. In the bone metastatic site, PCa cells secrete factors to stimulate matrix resorption and bone destruction, and cytokines (such as TGF-β) are released to facilitate PCa cells with active proliferation and dissemination capacities [8,9]. On the other hand, PCa cells produce multiple osteolytic mediators to cause further bone resorption and the so-called vicious cycle [10], among which parathyroid hormone-related protein (PTHrP) is probably the most important one, since approximately 90% of prostate cancer patients with bone metastases have elevated levels of PTHrP. Tumor cell derived PTHrP binds to its receptor PTHR1 on osteoblast and stimulates the osteoblast express receptor activator of nuclear factor κB ligand (RANKL), which is responsible for the induction of osteoclast differentiation and activation [11–15].

Bone metastatic prostate cancer cells highly express bone-related genes that contribute to osteomimetic characteristics [16]. Runt-related transcription factor 2 (Runx2, also known as Osf2/Cbfa1, AML3, or Pebp2αA), a crucial transcription factor in osteogenic commitment, is one of the most significant osteomimetic genes [17,18]. Runx2 plays important roles in prostate cancer bone metastasis *via* regulating the expression of RANKL, osteopontin (OPN), bone sialoprotein (BSP), vascular

Abbreviations: PCa, prostate cancer; DDR2, Discoidin domain receptor 2; PTHrP, Parathyroid hormone-related protein; MMP, matrix metalloproteinase

* Corresponding author at: 277 West Yanta Road, Xi'an Shaanxi 710061, PR China. Tel.: +86 29 85323528.

http://dx.doi.org/10.1016/j.bbadis.2014.04.018
0925-4439/

endothelial growth factor (VEGF), and matrix metalloproteinase 2, 9, 13 (MMP2, 9, 13) to participate in bone turnover [19,20]. Runx2 responds to TGF-β stimulation by up-regulating the expression of Indian hedgehog (IHH), which in turn increases the level of PTHrP [21]. Blockade of the Runx2-IHH axis in breast cancer cells by targeting Runx2 with short hairpin RNA prevents osteolytic disease [22].

Discoidin domain receptor 2 (DDR2) belongs to the receptor tyrosine kinase (RTK) family and is activated by collagen binding [23,24]. A unique feature that distinguishes DDR2 from other RTKs is that its activation by collagen is very slow and sustained (by hours), compared to the rapid response of typical RTKs to their ligands (by seconds to minutes) [24]. The main functions of DDR2 are to 1) control the remodeling of ECM by regulating the expression and activity of MMPs [25–27], 2) promote cell proliferation, adhesion and migration [28–32], 3) stimulate osteoblast differentiation and bone formation by regulation of the transcription activity and phosphorylation of Runx2 in an ERK MAPK-dependent manner [33,34]. In tumor, DDR2 participates in the process of melanoma liver metastasis [35], colorectal cancer metastasis [36], as well as the progression of nasopharyngeal carcinoma (NPC) [37], aneuploid papillary thyroid carcinomas [38], and breast carcinoma [39–41]. Furthermore, DDR2 is up-regulated by TGF-β and is involved in TGF-β-induced EMT in A549 lung cancer cells [42].

In the present study, we demonstrate that DDR2 is highly expressed in bone metastatic PCa cells and tissues, and is associated with increased motility and invasiveness of PCa cells. DDR2 promoted activation of osteoblast and osteoclast *in vitro* and boosted the formation of osteolytic lesions *in vivo*. We also elucidated the underlying mechanism that DDR2 regulates PTHrP *via* modulating the phosphorylation and transactivity of Runx2. In addition, DDR2 was involved in TGF-β-mediated bone resorption, and facilitated the adhesion of PCa cells to type I collagen. Our study aims to provide a novel potential target for PCa treatment in future.

2. Results

2.1. DDR2 is highly expressed in bone metastatic PCa cells and tissues

To investigate whether DDR2 participates in prostate cancer progression especially in bone metastasis, we examined the expression levels of DDR2 in normal prostate epithelial RWPE-1 and several PCa cells, including, brain metastatic DU145, lymph-node metastatic LNCaP, and bone metastatic MDA PCa 2b, VCaP, and PC-3. As shown in Fig. 1A, elevated mRNA levels of DDR2 were observed in PCa cells compared to normal prostate cells, and the mRNA level of DDR2 in bone metastatic cells was much higher than in the lymph-node or brain metastatic cells. Fig. 1B demonstrates that the protein levels of these cell lines were consistent with the RNA levels obtained from RT-PCR results. The protein level of DDR2 in PC-3 cells was approximately 3-fold compared to that of LNCaP cells. Furthermore, immunohistochemistry analysis in tissue samples revealed that DDR2 expression was detectable in 10.53% of benign prostatic hyperplasia (BPH) and high grade prostatic

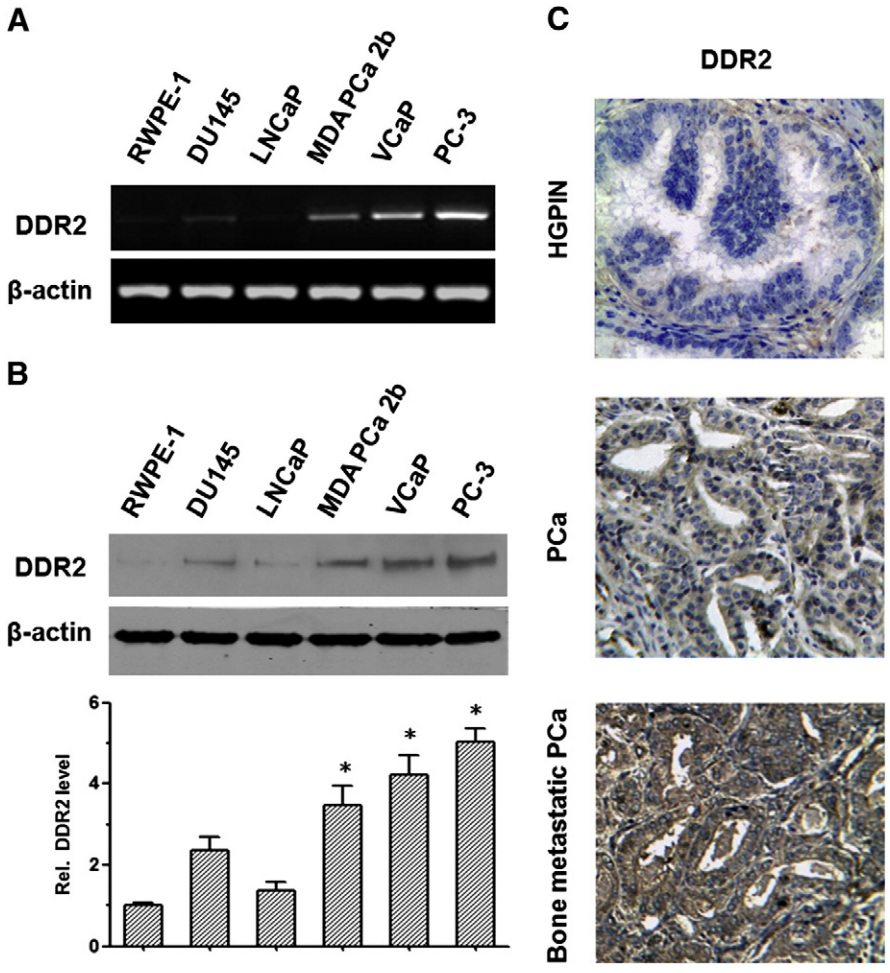

Fig. 1. DDR2 is highly expressed in bone metastatic PCa cells and tissues. (A) mRNA analysis of DDR2 in different cell lines. Cells were cultured in the indicated medium and were harvested for total RNA isolation. RT-PCR was carried out with the indicated primers. (B) Immunoblot analysis of DDR2 protein expression in different cell lines. The protein extracts were immunoblotted with the anti-DDR2 antibody, and β-actin was used for the loading control. Results were quantified using densitometry scanning and expressed as relative ratio compared to the RWPE-1 cells (right panel). *$p < 0.05$ *vs* RWPE-1 group. (C) Immunostaining for DDR2 in HGPIN and PCa specimens. Representative data are provided. Original magnification, ×400.

intraepithelial neoplasia (HGPIN) samples (2/19), but in 50% of the PCa samples without bone metastatic lesions (6/12) with relatively lower level, and in 100% of bone metastatic PCa samples (6/6) with much higher level. Representative data are shown in Fig. 1C. Collectively, these results implicated that DDR2 may have important roles in prostate cancer bone metastases.

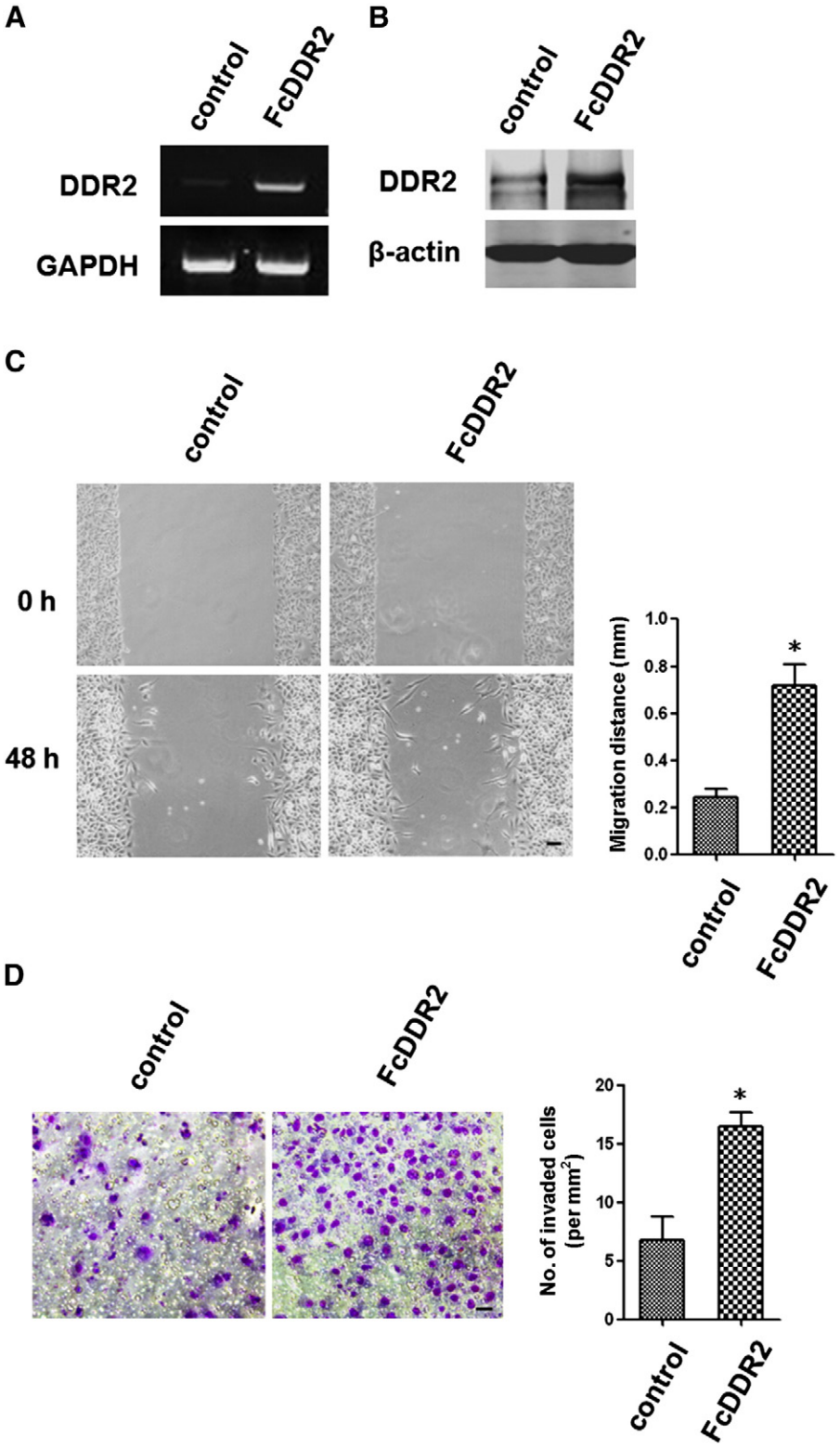

Fig. 2. DDR2 promotes PCa cells migration and invasion. (A) and (B) Confirmation of the efficiency of DDR2 over-expression. LNCaP cells were infected with lentivirus expressing FcDDR2 or GFP, the selected stable clone was analyzed for mRNA and protein expression level using RT-PCR and Western blotting. (C) DDR2 over-expression increases cell migration in wound healing assay. (D) DDR2 over-expression increases cell invasion in the Matrigel transwell chambers. Cells from 10 randomly chosen microscopic fields were counted, and cell invasion properties were expressed in terms of number of cells per mm^2. (E) and (F) Confirmation of the efficiency of DDR2 knock-down. PC-3 cells were infected with lentivirus expressing shRNA against *Ddr2* or scrambled shRNA, and the selected stable clone was analyzed by RT-PCR and Western blotting. (G) and (H) DDR2 deficiency leads to decrease in cell migration and invasion. Bar, 200 μm. *$p < 0.05$ *vs* control group.

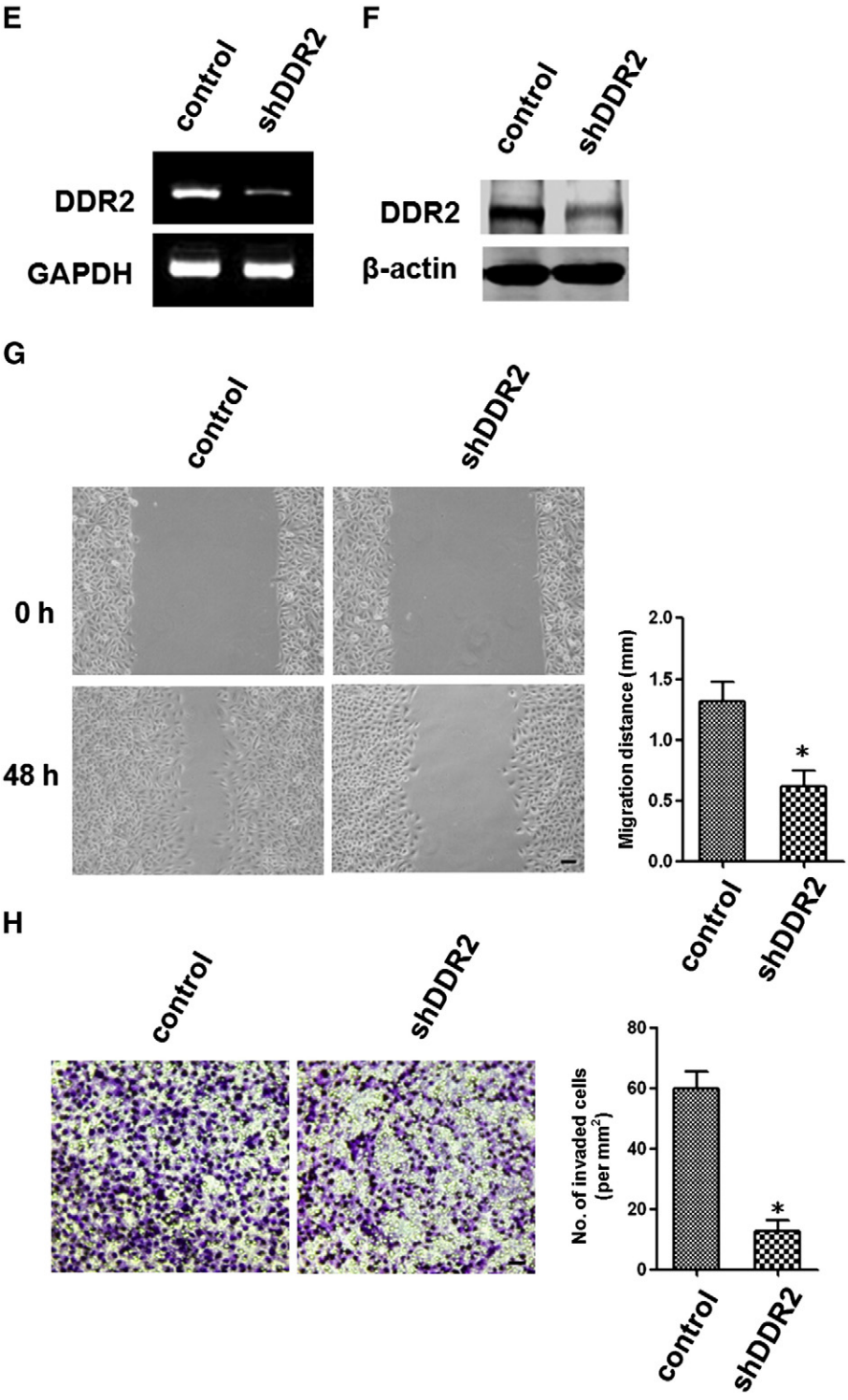

Fig. 2 (*continued*).

2.2. DDR2 promotes PCa cells migration and invasion

To define the role of DDR2 in prostate cancer bone metastases, we need to find out whether DDR2 has effects on the metastatic properties of PCa cells. DDR2 was over-expressed in LNCaP cells using lentivirus which expresses FcDDR2, a constitutively activated form of DDR2. Several clones were picked up and tested for the efficiency of over-expression using Western blotting (data not shown). The stable clone with the highest over-expression efficiency was selected, and its DDR2 expression level was significantly higher compared to that of the control clone (Fig. 2A and B). The migration and invasion abilities of FcDDR2-expressing and control cells were tested by monolayer wound healing assay and matrigel invasion assay. As shown in Fig. 2C, DDR2 over-expression resulted in an approximate 2-fold increase in the migration abilities of LNCaP cells. Fig. 2D also showed an elevation of about 1.4-time in the invasiveness of LNCaP cells after DDR2 expression level was enhanced.

In order to confirm our findings, we knocked down the DDR2 expression in PC-3 cells *via* specific shRNA against *Ddr2*. Scramble shRNA or shRNA against *Ddr2* was cloned into lentivirus packing vector and

the recombinant lentivirus were packaged and transducted into PC-3 cells to generate the stable control clones or *Ddr2*-knock down clones. As shown in Fig. 2E and F, the RNA and protein levels of DDR2 in the selected clone were reduced significantly compared to those in controls. Then their abilities of migration and invasion were analyzed, as shown in Fig. 2G and H, DDR2 knock-down suppressed the motility of PC-3

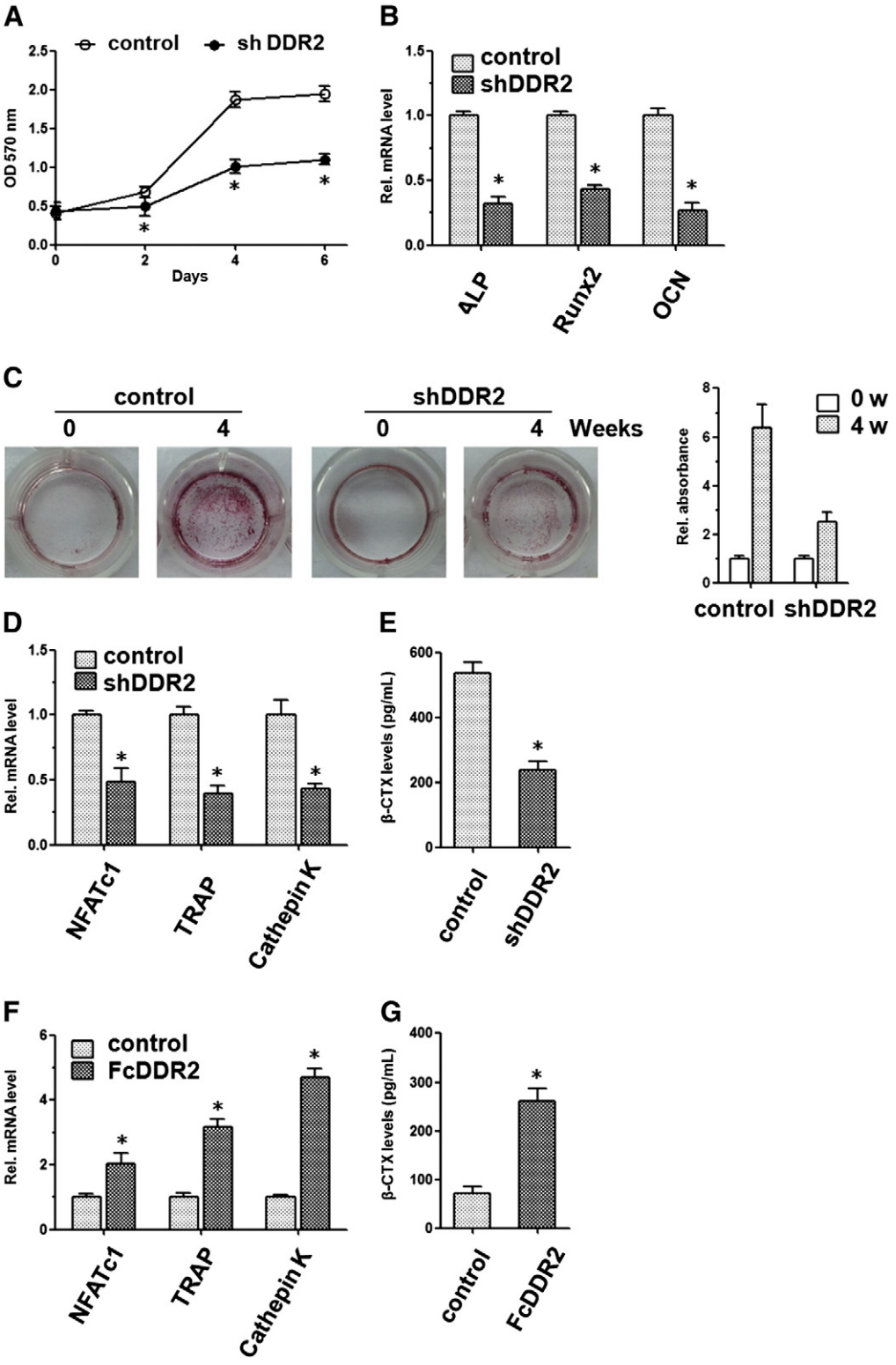

Fig. 3. DDR2 in PCa cells accelerates osteoblastogenesis and osteoclastogenesis in the co-culture system. (A) The proliferation of MC3T3-E1 cells was inhibited due to treatment with CM of DDR2 deficient MDA PCa 2b cells. CM of control or DDR2 knocked down MDA PCa 2b cells were collected to treat MC3T3-E1 cells, and cell proliferation was determined by crystal violet staining and subsequent acetic acid elution. (B) The differentiation of MC3T3-E1 cells was inhibited due to treatment with CM of DDR2 deficient MDA PCa 2b cells. Osteoblast differentiation was determined by detection of marker genes using real-time PCR. (C) The function of MC3T3-E1 cells was inhibited due to DDR2 deficient in MDA PCa 2b cells. The formation of mineralization nodules was determined by alizarin red staining. Osteoclast differentiation (D) and bone resorption (E) are retarded by treating with DDR2 silencing CM. Primary bone marrow cells were treated with CM from control and DDR2-silencing PC-3 cells, the mRNA levels of differentiation marker genes were analyzed and pit-formation assays were performed. Osteoclast differentiation (F) and bone resorption (G) are accelerated by treating with CM of DDR2 over-expressing LNCaP cells. *$p < 0.05$ vs control group.

cells by more than 50%, and an approximate 80% decrease of invasiveness occurred in response to DDR2 depletion.

2.3. DDR2 in PCa cells accelerates osteoblastogenesis and osteoclastogenesis in the co-culture system

After drawing the conclusion that DDR2 promotes prostate cancer metastases, we tried to elucidate the role of DDR2 in osseous metastasis, considering the high expression level of DDR2 in bone-metastatic PCa cells. We used osteoblastic MDA PCa 2b cells and osteolytic PC-3 cells to study the involvement of DDR2 in osteoblastic and osteolytic lesions respectively. The culture medium of control or DDR2-depleted MDA PCa 2b cells was collected to treat MC3T3-E1 cells. The proliferation of MC3T3-E1 cells was dramatically inhibited due to treatment with CM (conditioned medium) of DDR2 deficient MDA PCa 2b cells (Fig. 3A). The differentiation of MC3T3-E1 cells was retarded, determined by down-regulated expression of marker genes including ALP, Runx2, and OCN (Fig. 3B). The formation of mineralization nodules, an important indicator of osteoblast function, was also greatly affected after DDR2 was knocked down in MDA PCa 2b cells (Fig. 3C). These data suggested that DDR2 in MDA PCa 2b cells promoted the formation of osteoblastic lesions *in vitro*. As for the effect of DDR2 on the formation of osteolytic lesions, we collected the culture medium of control or DDR2-depleted PC-3 cells to treat primary bone marrow cells. Then osteoclast differentiation and bone resorption were tested using real-time PCR and pit formation assays. Expression of differentiation markers, such as NFATc1, TRAP, and Cathepsin K, were significantly decreased, suggesting the suppressed osteoclast differentiation caused by treatment with the CM of DDR2 silencing PC-3 cells (Fig. 3D). The osteoclast function and bone resorption were similarly inhibited, determined by the obvious decrease in β-CTX release (Fig. 3E). Then we used LNCaP cells, which form mixed lesions (osteoblastic/osteolytic) *in vivo*, to perform the co-culture assays for testing the involvement of DDR2 in LNCaP cells-mediated osteoblastogenesis and osteoclastogenesis. The enhanced osteoclast differentiation and bone resorption were detected when DDR2 was over-expressed in LNCaP cells (Fig. 3F and G). Taken together, these data demonstrated that DDR2 played an essential role in PCa cell-induced osteoblastogenesis and osteoclastogenesis, and participated in PCa osteoblastic and osteolytic metastases.

2.4. DDR2 promotes prostate cancer osteolytic metastasis in vivo

To validate our *in vitro* findings, we employed an intrabone injection bone metastasis mouse model to test the role of DDR2 in PCa bone metastasis. All control mice that received PBS injections did not develop osteolytic lesions at all. After 3 weeks, 1 of 12 mice that received PC-3 cell injection developed an osteolytic lesion, and 11 mice developed osteolytic lesions after 6 weeks, with a frequency of 91.7% (11/12). However, only 41.7% (5/12) of mice treated with DDR2-depleted PC-3 cells were found to have osteolytic lesions 6 weeks after injection, to a much slighter degree. The percentages of bone-metastatic-free animals in the three groups were shown in Fig. 4A. Representative X-ray images are shown in Fig. 4B.

2.5. DDR2 in PCa cells increase RANKL expression in osteoblasts to stimulate bone resorption

To find out why DDR2 affected osteoclastogenesis in addition to osteoblastogenesis, we tried to examine whether there was an indirect effect of osteoclast activation mediated by osteoblasts, since the cancer bone metastatic site is a microenvironment comprising cancer cells, osteoblasts, osteoclasts, osteocytes, and interaction between them, and the differentiation and activation of osteoclasts require co-stimulating factors provided by osteoblasts in PCa osteolysis lesions. We examined whether the secretion of RANKL or OPG in osteoblasts was affected by the change of DDR2 expression level in PCa cells. The culture medium of the control and DDR2 modified PCa cells was collected for treating MC3T3-E1 cells, and the expression of RANKL and OPG in MC3T3-E1

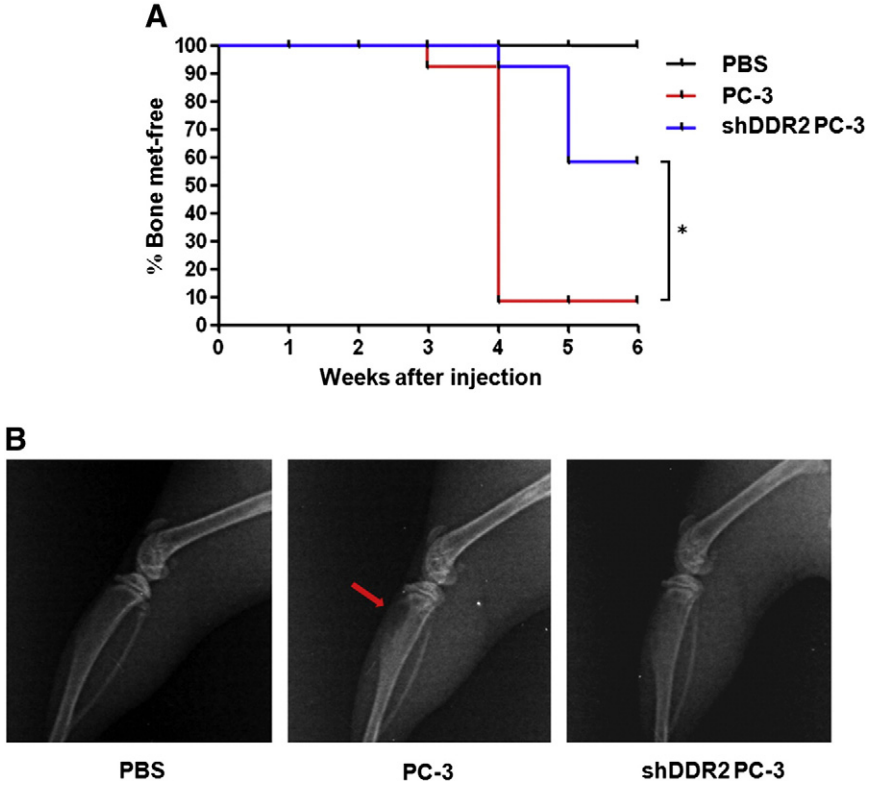

Fig. 4. DDR2 depletion alleviates PCa cells-induced osteolytic lesions. (A) Kaplan–Meier curve of bone metastasis development of control and DDR2-silencing PC-3 cells. N = 12. *$p < 0.05$ by log-rank test. (B). Representative X-radiographs (6 weeks) of mice from (A). Osteolytic lesion is marked by red arrow.

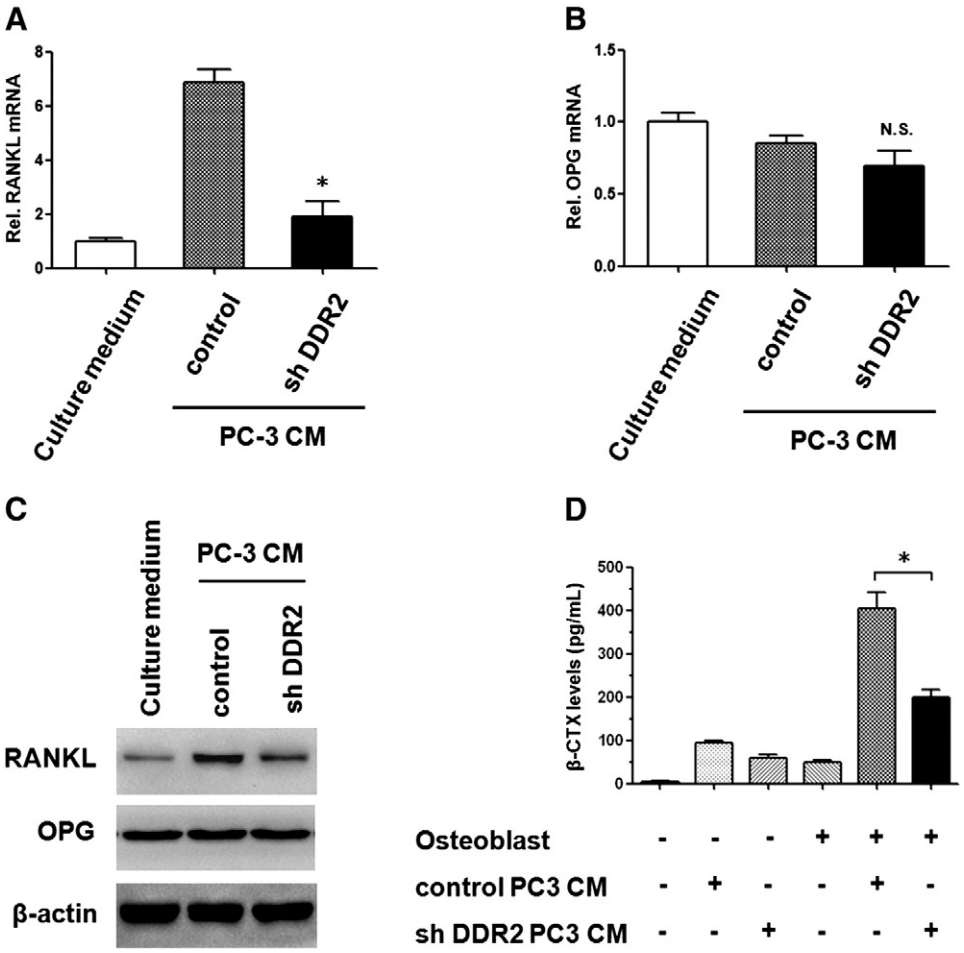

Fig. 5. DDR2 in PCa cells increases RANKL expression in osteoblasts to stimulate bone resorption. (A) and (B) The effect of DDR2 depletion on the mRNA level of RANKL and OPG. MC3T3-E1 cells were treated with CM from control and DDR2 over-expressing LNCaP cells. 5 d later the mRNA levels of the RANKL and OPG were analyzed. (C) The effect of DDR2 depletion on the protein level of RANKL and OPG. (D) Bone resorption was greatly suppressed in the presence of osteoblast. RAW264.7 cells were co-cultured with or without MC3T3-E1 cells in 10% DMEM containing 50% (v/v) CM, after 3 d of induction the culture supernatant was collected for assaying β-CTX. *$p < 0.05$ *vs* control of conditioned medium group; N.S. means non-significant.

cells was tested. As shown in Fig. 5A and B, the mRNA level of RANKL induced by the CM of DDR2 knock-down PC-3 cells was dramatically decreased, whereas the mRNA level of OPG has no obvious change. The protein levels of RANKL and OPG were consistent with the mRNA levels (Fig. 5C). In the presence of osteoblasts, the bone resorption was significantly suppressed when treated with CM of DDR2 deficient PC-3 cells (Fig. 5D). Similarly, the expression of RANKL was elevated (Fig. S1A) while that of OPG was reduced (Fig. S1B), due to the treatment of CM of DDR2 over-expressing LNCaP cells. The bone resorption was also dramatically stimulated in the presence of osteoblast (Fig. S1C). Collectively, these results implicated that DDR2 in PCa cells modulated RANKL expression of osteoblasts in a paracrine manner, and the DDR2-induced osteoclast activation and bone resorption were osteoblast-dependent.

2.6. DDR2 regulates PTHrP in PCa cells

To reveal the mechanism whereby DDR2 promoted PCa bone metastases, we tried to find out the DDR2-regulated genes involved in this regulation. The expression level of bone metastatic factors such as PTHrP, IL8, or IL11 were examined, since these genes were reported to up-regulate RANKL level of osteoblasts [11–15]. After DDR2 was modified, only expression of PTHrP was changed. As shown in Fig. 6A and B, DDR2 over-expression led to significantly enhancement of PTHrP expression, whereas DDR2 knockdown by specific siRNA resulted in dramatic impairment of PTHrP expression. The secretion of PTHrP in PC-3 cells was elevated to about 4-time due to DDR2 over-expression, and was remarkably attenuated due to DDR2 deficiency (Fig. 6C). Next, we detected the activity of PTHrP promoter using a pGL3-luc plasmid containing the sequence between −1450 and 300 nt around the transcription start site. As shown in Fig. 6D, the promoter activity of the DDR2 over-expressing cells was greatly increased, to a similar extent of Runx2 induction, while that of DDR2 deficient cells was remarkably decreased.

Runx2 is one of the known transcription factors regulating PTHrP expression. In our previous study, we proved that DDR2 modified the phosphorylation and transcriptional activity of Runx2 in osteoblasts and chondrocytes, so we wondered whether DDR2 could regulate PTHrP expression *via* modulation of Runx2 activation. To clarify the facts, we introduced a constitutively activated Runx2 vector, which contains Ser to Glu mutations and mimics the phosphorylation and transcriptional activation of Runx2 [43], into the stable DDR2-silenced PC-3 cells, to perform a rescue experiment. In Fig. 6E, we observed that introduction of Runx2 S301/319E mutant (with enhanced Runx2 phosphorylation) in shDDR2-transduced PC-3 cells rescued the decreased expression level of PTHrP caused by DDR2 deficiency, whereas an empty vector failed to show the rescue ability. Conversely, S301/319A Runx2 mutant, the inactivating Ser to Ala mutations with reduced phosphorylation and transcriptional ability of Runx2, led to a decrease in PTHrP expression (Fig. 6F). Taken together, these results demonstrated that DDR2 regulated the expression and secretion of PTHrP in PCa cells *via* affecting the phosphorylation of Runx2, and there was a DDR2-Runx2-PTHrP axis.

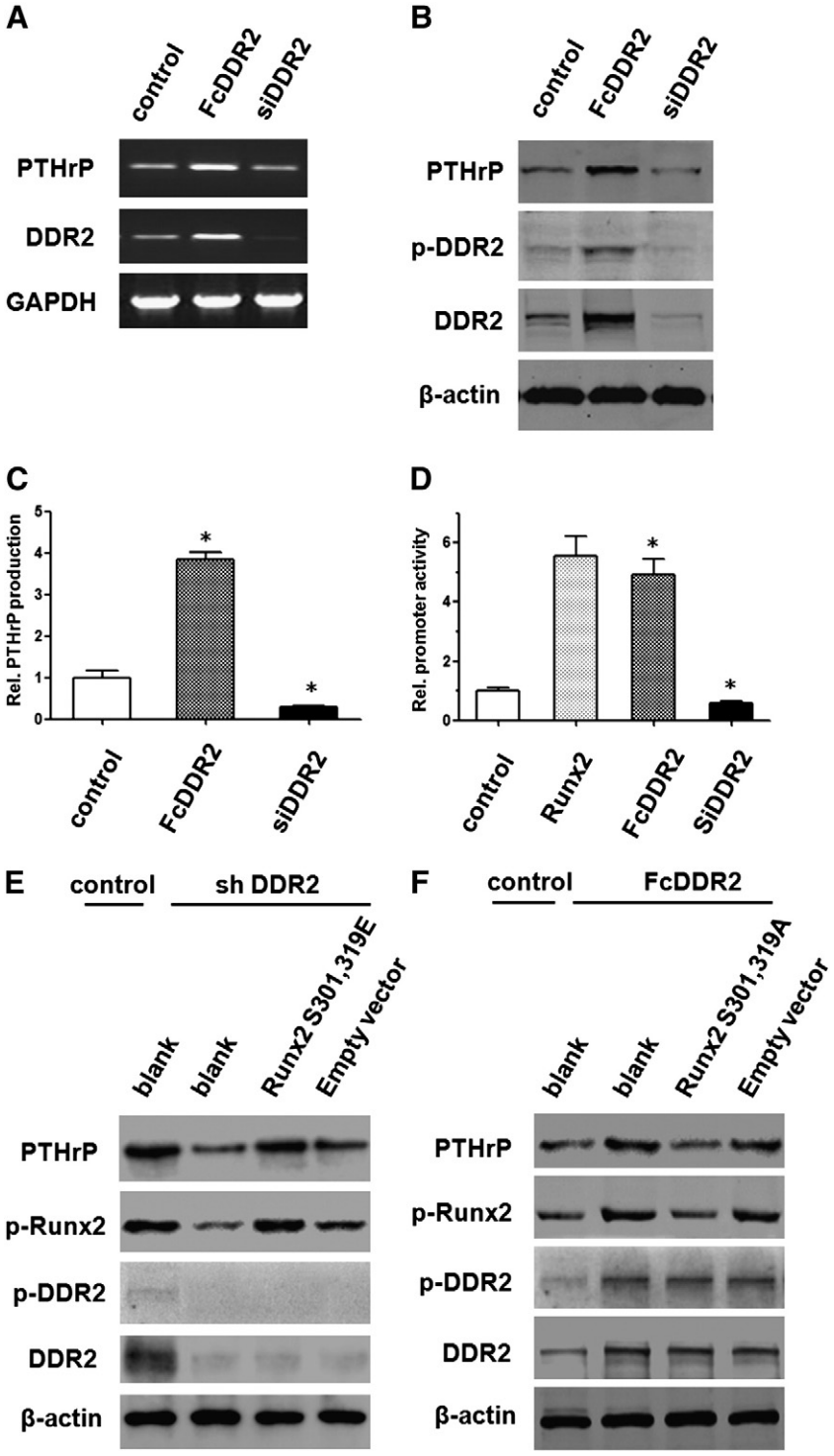

Fig. 6. DDR2 regulates PTHrP in PCa cells. (A) DDR2 regulates the mRNA level of PTHrP in PC-3 cells. Cells were transfected with FcDDR2 plasmid or siDDR2, 24 h later mRNA level of PTHrP were determined by RT-PCR. (B) DDR2 modulates the protein level of PTHrP in whole lysate of PC-3 cells. (C) DDR2 modulates the secretion of PTHrP in PC-3 cells. 48 h after the transfection, the culture medium was harvested for analyzing the secreted PTHrP level. (D) DDR2 regulates the promoter activity of PTHrP. 24 h after the transfection, pGL3-luc and phRL null vector were transfected into the cells, 48 h later the luciferase activities were assayed. (E) Constitutively activated mutation of Runx2 rescued the decreased PTHrP expression caused by the loss of DDR2. DDR2 knock-down PC-3 cells were transfected with empty vector or Runx2 S301/319E, 24 h later the cells were harvested and the protein level of PTHrP was tested by Western blotting. (F) Runx2 S301/319A abolished the FcDDR2 induction of PTHrP up-regulation. DDR2 over-expressing LNCaP cells were transfected with empty vector or Runx2 S301/319A, 24 h later the cells were harvested and the protein level of PTHrP was tested by Western blotting. *$p < 0.05$ *vs* control group.

2.7. DDR2 is responsive to TGF-β stimulation to function as a bone metastasis inducer

We have proved in the above section that DDR2 promotes prostate cancer bone metastasis by inducing PTHrP secretion *via* modulation of Runx2 phosphorylation. However, there are still some questions that need to be answered. How does the up-regulation of DDR2 in expression or activity occur? Which molecule triggers DDR2 in the process of bone metastasis? Given that TGF-β is one of the most important mediators in the prostate cancer microenvironment and the vicious cycle

between cancer cells and bone cells, we investigated the responsiveness of DDR2 to TGF-β and tried to find out whether TGF-β facilitates the bone metastasis promotion effect of DDR2. As shown in Fig. 7A, after treatment of TGF-β, the protein level of DDR2 in PC-3 cells was increased significantly, followed by an enhancement of phosphorylation level of Runx2 and expression level of PTHrP.

Then we detected the transcriptional activity of Runx2 to see if it is affected by TGF-β treatment. The specificity of the probe for Runx2 is verified by cold probe competition assay and antibody-binding super-shift assay (Fig. 7B, lanes 1–6). When a labeled wild-type probe was incubated with the nuclear extracts from LNCaP cells, a band shift was detected, indicating that the nuclear proteins effectively bound and formed a complex with the probe (Fig. 7B, lanes 1 and 2). The addition of 300-fold excess of unlabeled wild-type but not mutant probe abolished the formation of the protein–DNA complex (Fig. 7B, lanes 3 and 4). Furthermore, a super-shift band was observed above the previous band shift when the nuclear extracts were pre-incubated with an antibody against Runx2 but not unimmunized goat IgG (Fig. 7B, lanes 5 and 6). Hence the probe in this system is specific for Runx2 binding. As shown in Fig. 7B (lanes 7 and 8), the DNA binding ability of Runx2 in LNCaP cells was significantly elevated after being treated by TGF-β.

Finally, we detected the amount of PTHrP secreted to the culture medium using ELISA. As shown in Fig. 7C, the production of PTHrP in PC-3 cells was approximately 4-time higher when treated with TGF-β, whereas the up-regulation was not so obvious in DDR2-silencing PC-3 cells. We co-cultured the PC-3 cells with MC3T3-E1 cells and detected the mRNA level of RANKL in MC3T3-E1 cells. As shown in Fig. 7D, The mRNA of RANKL was dramatically induced after adding TGF-β to the condition medium, whereas DDR2-silencing PC-3 cells were not as responsive as the control cells. The function of osteoclasts and osteoclastogenesis was obviously accelerated by TGF-β treatment and at least partly, DDR2 contributes to this effect (Fig. 7E).

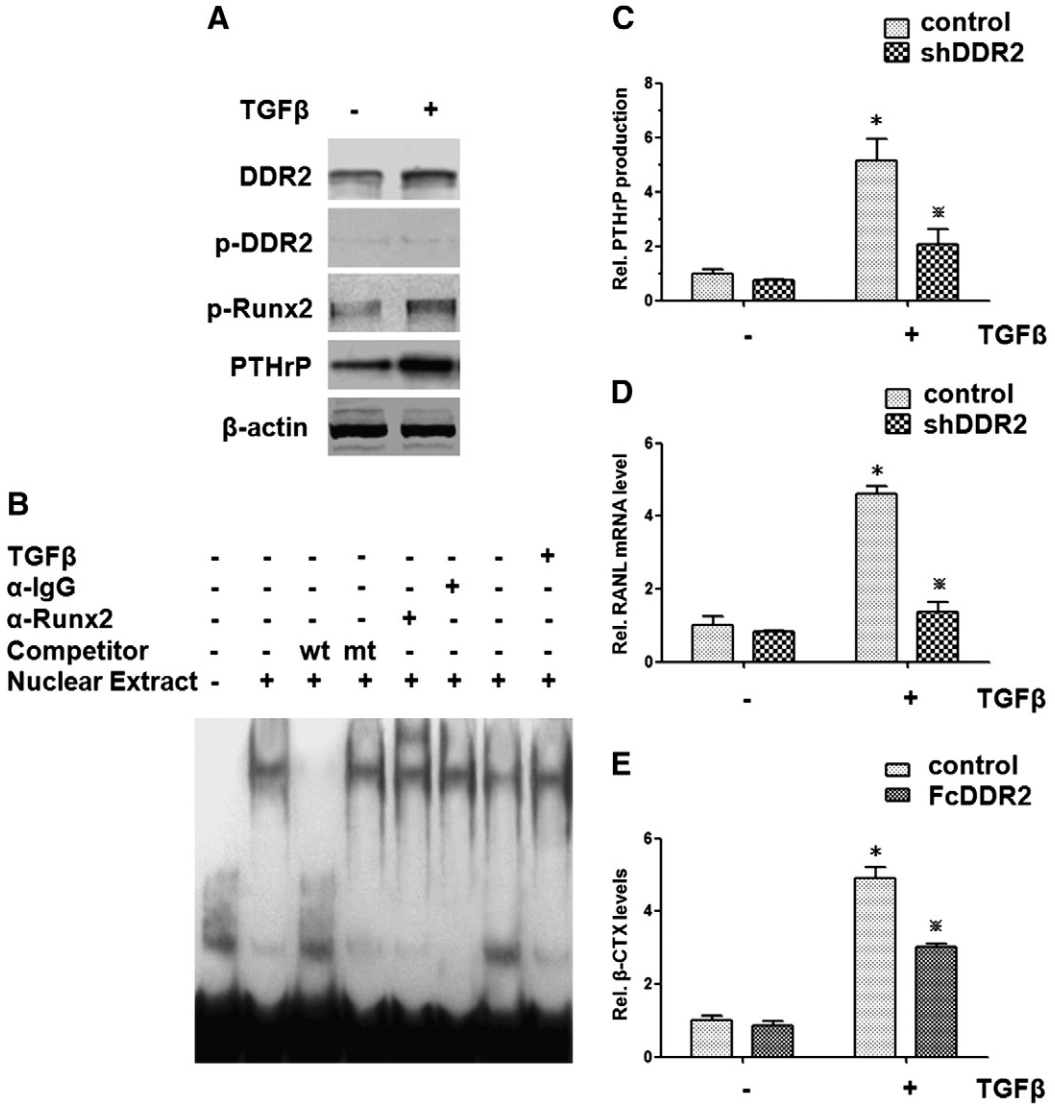

Fig. 7. DDR2 is responsive to TGF-β stimulation. (A) TGF-β treatment leads to up-regulation of DDR2 expression, Runx2 phosphorylation, and PTHrP production. PC-3 cells were serum starved before being treated with or without 200 ng/mL TGF-β1 for 48 h. The expression levels of indicated protein were determined by Western blotting. (B) The transactivity of Runx2 is stimulated by TGF-β. LNCaP cells were treated as described in (A), and the nuclear protein was extracted and the DNA binding abilities of Runx2 were assayed by EMSA. (C) TGF-β induces the production of PTHrP *via* DDR2 in PC-3 cells. PC-3 cells were treated with 200 ng/mL of TGF-β1 for 48 h and the culture medium was collected for PTHrP quantification by ELISA. (D) DDR2 mediated the up-regulation of RANKL expression induced by TGF-β. The CM from DDR2-silencing and control cells were harvested and added to the culture medium of MC3T3-E1 and the mRNA level of RANKL in MC3T3-E1 was detected by real-time PCR. (E) The activities of osteoclasts were enhanced by TGF-β and DDR2 was involved in this regulation. Primary bone marrow cells were treated with CM from DDR2 over-expressing and control cells as described above, pit formation assay was performed. *$p < 0.05$ *vs* control in the TGF-β-free group; $p < 0.05$ *vs* control in the TGF-β-treated group.

2.8. DDR2 facilitates the binding of PCa cells to type I collagen

Given that DDR2 could be bound and activated by type I collagen, which makes up more than 90% of the total protein within the bone, we detected the binding abilities of PCa cells to collagen I owing to DDR2. As shown in Fig. 8A, bone metastatic PC-3 and VCaP cells, which express high levels of DDR2 (Fig. 1), had stronger abilities to bind collagen I, with an about 4-time increase compared to non-bone metastatic PCa cells, whereas there was no difference in their abilities of binding to fibronectin. Then the effect of DDR2 on specific binding to collagen I was tested. As indicated in Fig. 8B, over-expression of DDR2 in LNCaP cells led to a significant elevation in specific binding of collagen I, whereas depletion of DDR2 in PC-3 cells resulted in a dramatic decline. To further confirm the specific role of DDR2, recombinant DDR2 protein was used to block the function of DDR2, and the binding abilities of LNCaP and PC-3 cells to type I collagen were analyzed. As shown in Fig. 8C, when pre-incubation of recombinant DDR2 protein was carried out, the binding of PC-3 cells to type I collagen dropped dramatically to approximately one-half. However, no obvious change in fibronectin-binding was observed after the recombinant DDR2 protein pre-incubation.

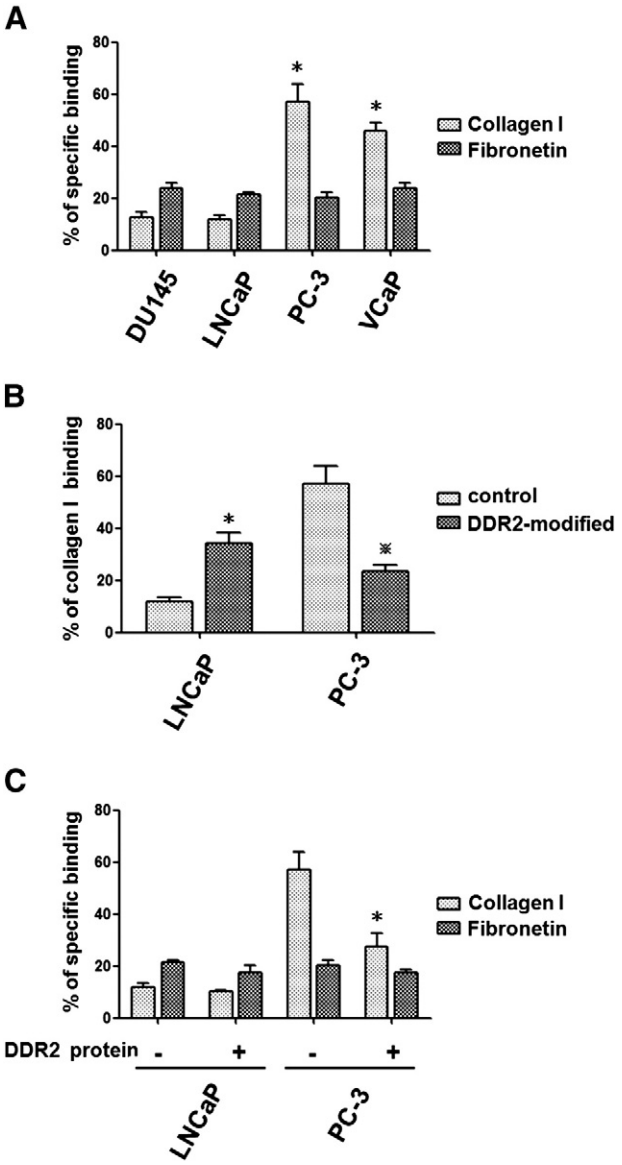

Fig. 8. DDR2 facilitates the adhesion of PCa cells to collagen I. (A) Collagen I binding abilities of PCa cell lines. Collagen I, fibronectin or BSA was coated on cell culture dishes, and PCa cells were seeded on the pre-coated dishes for performing the cell adhesion assay. The percentage of specific binding to either type I collagen or fibronectin was calculated by subtracting the mean nonspecific binding to BSA. *$p < 0.05$ *vs* collagen I-treated DU145 or LNCaP group. (B) Effect of DDR2 on collagen I binding abilities. DDR2 over-expression in LNCaP led to increase in collagen I binding, whereas DDR2 knock down in PC-3 cells resulted in decrease. *$p < 0.05$ *vs* control LNCaP group; $p < 0.05$ *vs* control PC-3 group. (C) Pre-incubation of recombinant DDR2 protein impaired the binding of PC-3 cells to collagen I. 10 μg/mL recombinant DDR2 protein was pre-incubated for 45 min at 37 °C, and specific binding was assayed. *$p < 0.05$ *vs* DDR2-free collagen I-treated PC-3 group.

Taken together, the role of DDR2 in prostate cancer bone metastasis could be displayed in the schematic diagram (Fig. 9). TGF-β in tumor microenvironment stimulates DDR2 expression. DDR2 facilitates the specific binding of PCa cells to collagen I, which is the main component of bone. In the bone metastasis site, up-regulation of DDR2 expression and activation leads to phosphorylation and activation of Runx2, as well as the following release of PTHrP. Osteoblastogenesis was provoked by PTHrP and meanwhile osteoblasts expressed more RANKL to accelerate osteoclast differentiation and bone resorption. Thus DDR2 contributed to both osteoblastic and osteoclastic lesions in bone metastasis.

3. Discussion

Prostate cancer dissemination and skeletal metastases represent major therapeutic challenges. Once the skeletal metastasis occurs, the incurable patient could just be symptomatically treated to alleviate the pain. Therefore it is of great necessity to disclose the molecular mechanisms underlying PCa metastasis and its propensity for bone, as well as uncovering the potential targets for future research. We found that the expression level of DDR2 was significantly higher in bone metastatic PCa cells and tissues, which prompted us to investigate the role of DDR2 in PCa dissemination and bone metastases. DDR2 has been implicated in playing essential roles in other cancer types but PCa. Our previous study suggested the function of DDR2 in the regulation of the transactivity and phosphorylation of Runx2, a key regulator of PCa bone metastasis. Based on these findings, we hypothesized that DDR2 promotes PCa metastasis and bone-homing *via* Runx2 regulation.

In the present study, we initially observed that the expression level of DDR2 was notably elevated in the bone metastatic PCa cells and tissues, compared with normal and non-bone-metastatic controls. DDR2 positively regulated the migration and invasion abilities of PCa cells. DDR2 in PCa cells stimulated osteoblastogenesis and osteoclastogenesis

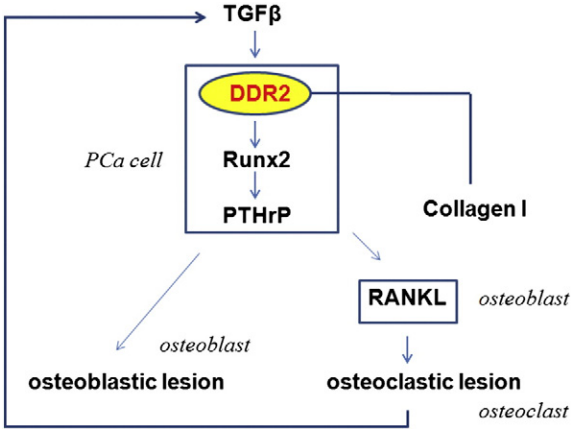

Fig. 9. A schematic model depicting molecular mechanisms underlying DDR2-mediated prostate cancer bone metastasis. TGF-β in tumor microenvironment stimulates the expression of DDR2, which is responsible for the Runx2 activation and subsequently PTHrP secretion. In bone metastasis site, PTHrP promotes osteoblast proliferation, differentiation and function, at the same time DDR2 stimulates RANKL expression in osteoblasts, leading to the activation of osteoclasts and enhanced osteoclastogenesis. Furthermore, DDR2 facilitates the specific binding of PCa cells to collagen I, which is the main component of bone.

in vitro, and DDR2 depletion alleviated osteolytic lesions *in vivo*. The underlying mechanism was that DDR2 in PCa cells regulated the expression, secretion, and promoter activity of PTHrP *via* regulating the transactivity and phosphorylation of Ruxn2, to affect the RANKL expression of osteoblasts, which in turn stimulated osteoclast activation and bone resorption. Moreover, DDR2 was responsive to TGF-β stimulation and participated in the TGF-β-induced bone resorption. DDR2 also mediated the adhesion of PCa cells to type I collagen, the main component of bone.

DDR2 has been implicated in the progression of several types of cancer. DDR2 participates in the liver metastasis of melanoma, contributes to colorectal dissemination by increasing myofibroblasts, neoangiogenic vessels and proliferating cancer cells. DDR2 is closely associated with nasopharyngeal carcinoma (NPC) and aneuploid papillary thyroid carcinomas, and is involved in EMT of several types of cancer cells including breast and lung cancer cells using distinct mechanisms. Activated mutation of DDR2 was also found in lung squamous-cell carcinoma. However, there is another report regarding the negative regulatory role of DDR2 in tumor progression (DDR2 deficiency predisposes hepatic tissue to colon carcinoma) [44], suggesting that the role of DDR2 in tumors is complicated and cellular context dependent. Until now there is no literature reporting the roles of DDR2 in PCa and PCa bone colonization. Our original study implicates DDR2 in PCa bone metastasis for the first time and is of great significance for the future treatment of prostate cancer. Moreover, the target genes downstream of DDR2 are largely unknown, and the detailed signaling pathways mediating DDR2 regulation of target gene transcription are poorly understood. In the present study, we demonstrated that PTHrP is regulated by DDR2 in PCa cells. This finding expands the DDR2-Runx2 axis to TGFβ-DDR2-Runx2-PTHrP pathway.

Prostate cancer bone metastases result in mixed, heterogeneous osteoblastic and osteolytic lesions. Osteoblastic lesions are characterized by excess deposition of new bone, whereas osteolytic lesions are characterized by the destruction of bone. These two types of PCa bone metastases all cause disturbance of bone microenvironment homeostasis. PCa cells secrete factors that stimulate the proliferation and differentiation of osteoprogenitor cells, or induce osteoclast precursors differentiate into mature osteoclasts in the tumor environment. Although clinically osteoblastic lesions account as a major component, there are still existing osteolytic lesions which are due to the activation of osteoclasts. It is unknown which kind of bone metastatic lesions, osteoblastic or osteolytic, occur initially. In our study, we demonstrated that the formation of osteolytic lesions required osteoblasts, suggesting the initiating role of osteoblastic lesions in PCa bone metastases. DDR2 acted as a stimulator for PCa bone metastases *via* regulating PTHrP, which has been implicated to function in an autocrine, paracrine or intracrine manner. Here we only discussed the paracrine manner of PTHrP to influence the bone microenvironment. Other aspects of PTHrP function, such as stimulating cell proliferation, adhesion and survival by directly acting on tumor cells, were not investigated in this study. Our results showed that PCa cell-derived PTHrP was responsible for the stimulated osteoblast proliferation and activation, as well as the promoted osteoclast differentiation and bone resorption, being consistent with previous reports [45].

In the process of PCa cells metastasizing to the bone, PCa cells produce MMPs and other enzymes to degrade the basement membrane and invade the bloodstream from the primary site. Based on our previous studies, DDR2 activation led to the secretion and activation of MMP2, 13 (Fig. S2). So we speculated that in the early stage of PCa bone metastasis, DDR2-MMPs axis accounts for a larger contribution. Then the circulating PCa cells with high DDR2 expression levels are specifically attracted by type I collagen, which is the most abundant extracellular matrix protein in bone. In the bone metastatic site, PTHrP is stimulated by DDR2 activation and acts on osteoblasts to stimulate osteoblast differentiation and bone formation, or accelerate the differentiation of osteoclasts and bone resorption. TGF-β is then released from the bone reservoir and regulates the expression of DDR2. Thus, DDR2 acts an important mediator in the vicious cycle of tumor cell proliferation and bone destruction. Collectively, DDR2 functions at different levels (invasion, homing, pro-osteoblastic, pro-osteoclastic) to promote PCa bone metastasis.

However, there are still some issues that remain poorly understood. For instance, how TGF-β modulates DDR2 expression and whether Smads participate in the regulation. How does DDR2 regulate the expression of PTHrP *via* Runx2? Is there any other kinase downstream of DDR2 participating in PTHrP regulation, such as p38? These questions would be answered in our future studies.

4. Materials and methods

4.1. Antibodies and reagents

The antibodies used in this study were as follows: goat anti-DDR2 (R&D Systems, MN, USA), rabbit anti-Runx2 S533 (Epitomics, CA, USA), goat anti-PTHrP (Santa Cruz, CA, USA). Recombinant human TGF-β1, recombinant murine M-CSF and sRANKL were purchased from Peprotech (NJ, USA). Ascorbic acid (AA) and β-glycerophosphate (β-GP) were purchased from Sigma (Shanghai, China), Type I collagen and fibronectin were purchased from BD Biosciences (MA, USA). Recombinant human DDR2 protein was purchased from Abnova (CA, USA). The Runx2 S301/319E and Runx2 S301/319A plasmid were described previously [33]. The −1450 to 300 of PTHrP gene (PTHLH) promoter were amplified by PCR and inserted into pGL3-luc vector (Promega, WI, USA) using *Kpn* I and *Xho* I.

4.2. Cell culture

Normal prostate epithelial RWPE-1 was cultured in K-SFM (Invitrogen, CA, USA) supplemented with 50 μg/mL bovine pituitary extract (BPE), 5 ng/mL EGF and 10% fetal bovine serum (FBS). PCa cell lines LNCaP, DU145, MDA PCa 2b, PC-3 and VCaP were cultured in Dulbecco's modified essential medium (DMEM) supplemented with 10% FBS. Murine RAW264.7 cells and primary bone marrow cells were cultured in DMEM supplemented with 10% FBS. Murine pre-osteoblast cell MC3T3-E1 (subclone 14) were cultured in α-minimal essential medium (α-MEM, Invitrogen, CA, USA) with 10% FBS. All cells were maintained in a humidified atmosphere with 5% CO_2 at 37 °C.

4.3. Immunohistochemistry

This study was approved by the Ethics Committee of The First Affiliated Hospital of Xi'an Jiaotong University College. Nineteen BPH and HGPIN samples and 18 PCa samples (6 cases with bone metastatic lesions) were fixed in 10% neutralized formalin and embedded in paraffin blocks. Sections (4 μm) were prepared for the evaluation of DDR2 expression. For immunohistochemical analysis, the endogenous peroxidase activity was blocked using 3% H_2O_2 for 1 h, followed by incubation with 5% Serum-Free Protein Block and then primary antibody anti-DDR2 (1:100) at 4 °C overnight. Immunodetection was performed in a 3-step protocol, using streptavidin-horseradish peroxidase complex, with visualization by 3,3-diaminobenzidine.

4.4. Co-culture assay

Cell conditioned medium (CM) was collected from DDR2 modified PCa cells. The medium was harvested, sterile filtered and stored at −20 °C until needed. In co-culture assay, MC3T3-E1 cells were seeded at the density of $5 \times 10^4/cm^2$, and cultured in 10% α-MEM supplemented with 50% (v/v) CM in the presence of osteogenic inducers: 50 mg/mL AA and 5 mM β-GP. Alternatively primary bone marrow cells were seeded at the density of $4 \times 10^3/cm^2$, and cultured in 10% DMEM supplemented with 50% (v/v) CM, in addition with 50 ng/mL M-CSF and

100 ng/mL RANKL. The medium was replaced every 48 h, at the indicated time point the differentiation was determined by real-time PCR detection of mRNA levels of marker genes.

4.5. Lentivirus packaging and infection

The lentivirus system for short hairpin RNA (shRNA) expression included three plasmids (pLKO.1, psPAX2, and pMD2.G) and was obtained from Addgene (Cambridge, MA, USA). Sense and antisense shDNA oligos were annealed and ligated into the pLKO.1 vector, generating plasmids that expressed shRNA against DDR2 or a scramble RNA respectively. FcDDR2 was inserted into the lentivirus shuttle vector designed for cDNA expression. Then 3×10^5 HEK-293 T cells at 70% confluence were transfected with 1 μg of shuttle vector, 750 ng of psPAX2, and 250 ng of pMD2.G using Lipofectamine^{2000} (Invitrogen, CA, USA). Twelve hours after transfection, the medium was changed. Cells were cultured for an additional 36 h before the culture medium was harvested. Once target cells reached 50% confluence, they were incubated with virus-containing medium for 48 h and further grown in medium containing 6 μg/mL of puromycin (Invitrogen, CA, USA). After 3 weeks of selection, single colonies were picked up and tested for their expression level of DDR2. The most efficient modified clone was used for further studies.

4.6. Quantitative real-time PCR analysis

Total RNA was extracted using Trizol (Invitrogen, CA, USA). Complementary DNA (cDNA) was synthesized from 2 μg of total RNA using the Super-Script II First-Strand Synthesis System (Invitrogen, CA, USA). The mRNA levels were determined either by semiquantitative reverse-transcriptase PCR (RT-PCR) or by quantitative real-time PCR. The glyceraldehyde-3-phosphate dehydrogenase (*Gapdh*) gene was used as an endogenous control. The sequences of primers for various genes are shown in Table 1. Details of the reaction system and amplification procedure were described previously [33].

4.7. Western blotting

Cells were lysed with radioimmunoprecipitation assay (RIPA) buffer supplemented with protease inhibitors (Roche, NJ, USA). Protein lysates were subjected to 10% SDS-PAGE, transferred to nitrocellulose membrane (Bio-Rad, CA, USA), and incubated with the indicated antibody. Bands were developed with enhanced chemiluminescence (ECL) system (Amersham Bioscience, UK). The blots were reprobed with β-actin antibody for the loading control.

Table 1
Prime sequences for PCR analysis.

Gene		Primer sequence
Ddr2	Forward	5′-CTCCCAGAATTTGCTCCAG-3′
	Reverse	5′-GCCACATCTTTTCCTGAGA-3′
Alp	Forward	5′-TTGTGCGAGAGAAAGGAGA-3′
	Reverse	5′-GTTTCAGGGCATTTTTCAAGGT-3′
Runx2	Forward	5′-CGCCCCTCCCTGAACTCT-3′
	Reverse	5′-TGCCTGCCTGGGATCTGTA-3′
Ocn	Forward	5′-CTGACTGACAAAGCCTTCATGTCCAA-3′
	Reverse	5′-GCGCCGGAGTCTGTTCACTA-3′
Rankl	Forward	5′-GCTGGGCCAAGATCTCTAAC-3′
	Reverse	5′-GTAGGTACGCTTCCCGATGT-3′
Opg	Forward	5′-ACTGGTCATCAGCTCCTGTG-3′
	Reverse	5′-TGTCTTCCTCCTCACTGTGC- 3′
Pthlh,	Forward	5′-GAGACTGGTTCAGCAGTGGA-3′
	Reverse	5′-TGTCATGGAGGAGCTGATGT-3′
Nfatc1	Forward	5′-ATACCTGGCTCGGTAACACC-3′
	Reverse	5′-CATGCTCCAGTGCTGTCTTT-3′
CathepsinK	Forward	5′-CACTGGATAATTAAAAACAGCTGGG-3′
	Reverse	5′-CCAGGTTGGCAATGCCAC-3′
Trap	Forward	5′-TCTCCAAGCGCTGGAACTTC-3′
	Reverse	5′-CATTGGTCTGTGGGATCTTGAA-3′
Gapdh	Forward	5′-TTCGACAGTCAGCCGCATCTTCTT-3′
	Reverse	5′-CAGGCGCCCAATACGACCAAATC-3′

4.7.1. Cell proliferation assay

MC3T3-E1 cells were plated in 24-well plates (5×10^3/well) in quadruplicate and cultured in the culture medium supplemented with 50% CM of control or DDR2-depleted MDA PCa 2b cells. At the indicated time point, cells were fixed for staining with 0.5% (w/v) crystal violet. Destaining was carried out with 35% (v/v) acetic acid and the absorbance was read at 570 nm. The optical density was used to represent the relative cell number.

4.7.2. Alizarin red staining

Cells were fixed with 95% ethanol, and then further treated with 40 mM alizarin red stain (AR-S) solution (pH 4.2) for 30 min to label the calcium deposits. The stained cultures were photographed, and the AR-S was extracted with 10% (w/v) cetylpyridinium chloride in 10 mM sodium phosphate (pH 7.0). The AR-S concentration was determined by measuring the absorbance at 540 nm using an AR-S standard curve.

4.8. Luciferase report assay

Cells were transiently transfected with 1 μg pGL3-luc reporter vector plus 0.05 μg pRL-null Renilla luciferase vector (Promega, WI, USA) using Roche Transfection reagents, 48 h later cell lysates were harvested and the luciferase activity in the cell lysates was assayed using the Dual Luciferase Reporter Kit (Promega, WI, USA). Transfections were performed in triplicate and normalized to Renilla luciferase activity.

4.9. Electrophoretic mobility shift assay

Electrophoretic mobility shift assay (EMSA) was performed according to the kit procedure (Pierce, IL, USA). Nuclear extracts were prepared using the NE-PER nuclear and cytoplasmic extraction reagents (Pierce, IL, USA). The sequences of probes are shown in Table 2. Nuclear proteins (3 μg) were incubated with 20 fmol of biotin-labeled wt-probe or mt-probe, and the DNA–protein complex was separated on a 6% nondenaturing polyacrylamide gel in 0.5× TBE with 2.5% glycerol and transferred to positively charged nylon membranes. The membranes were blocked with blocking buffer and incubated with HRP-conjugated streptavidin. The blots were developed with chemiluminescence substrate solution (Pierce, IL, USA) and exposed to X-ray film. For competition assays, 300-fold excess of unlabeled probes were added to the reaction mixture for 30 min at room temperature before the addition of the labeled probe.

4.10. Wound healing assay

Cells were cultured in 35 mm dishes with DMEM containing 10% FBS until they reached subconfluence, then the monolayer was scratched with a 200 μL pipette tip. Cells were washed with PBS twice and cultured in FBS-free medium for additional 48 h. Cell migration into the

Table 2
Probe sequences for EMSA.

Probe	Probe sequence
wt-Probe	5′-CCCAGGCAGCTGCAATCACCAACCACAGCATCCTTTGGGTTTGAC-3′
	5′-GTGGGTCAAACCCAAAGGATGCTGTGGTTGGTGATTGCAGCTGCC-3′
mt-Probe	5′-CCCAGGCAGCTGCAATCACCAAGAACAGCATCCTTTGGGTTTGAC-3′
	5′-GTGGGTCAAACCCAAAGGATGCTGTTCTTGGTGATTGCAGCTGCC-3′

Note: The underlined characters indicate the mutation site. A 5′-biotin modification was included in all probes except for the competitor oligonucleotides, which did not contain any modification. wt: wild type; mt: mutant type.

wound area was monitored by inverted microscopy, photographed at the indicated time point, and analyzed using Leica LAS EZ software. The distance of cell migration was calculated as the migration distance (mm) by subtracting the distance between the lesion edges at 48 h from the distance measured at 0 h.

4.11. Cell invasion assay

Cell invasion experiments were performed using Bio-Coat cell migration chambers (BD Biosciences, MA, USA), which consist of a 24-well companion plate with cell culture inserts containing a filter with 8 μm-diameter pores. Filters were coated with basement membrane Matrigel (40 μg/filter). Cells resuspended in DMEM/BSA medium (3×10^5 cells/500 μL) were added to the insert (upper chamber), and DMEM containing 20% FBS was placed in the lower chamber (800 μL/well). After incubation at 37 °C for 48 h, the upper surface of the membrane was wiped with a cotton-tipped applicator to remove non invading cells, the invading cells on the under surface were fixed with 5% glutaraldehyde fixative and stained with Giemsa. Cells from 10 randomly chosen microscopic fields were counted and cell invasion was expressed in terms of number of cells per mm^2.

4.12. Cell adhesion assay

Cells were seeded on 1 $\mu g/cm^2$ Collagen I, fibronectin or BSA-coated dishes, which were pre-treated by the removal of excess protein and blocking with medium containing 1% BSA for 1 h at 37 °C. After a 2 h incubation at 37 °C, nonadherent cells were removed, and adherent cells were fixed and stained with 0.5% (w/v) crystal violet. Destaining was carried out with 35% (v/v) acetic acid and the absorbance was read at 570 nm. The percentage of specific binding to either type I collagen or fibronectin was calculated by subtracting the mean nonspecific binding to BSA. To characterize the specific role of DDR2, the adhesion assay was followed by a 45-minute, 37 °C preincubation of the 10 μg/mL recombinant DDR2 protein.

4.13. Pit formation assay and β-CTX quantification

Mouse primary bone marrow cells or RAW264.7 cells were seeded on the BioCoat™ Osteologic™ dishes (BD Biosciences, MA, USA) at the density of $4 \times 10^3/cm^2$ and cultured in 10% DMEM containing 50% (v/v) CM, 50 ng/mL M-CSF, and 100 ng/mL RANKL. Alternatively, RAW264.7 cells and MC3T3-E1 cells were co-cultured at the ratio of 1:1 in 10% DMEM containing 50% (v/v) CM. The medium was replaced every other day, and after 3 d of induction the culture supernatant were collected and assayed for the amount of β-CTX, which was used to indicate the extent of bone resorption. The procedure of β-CTX quantification was as described in the manufacturer's instructions (Elabscience Biotechnology, China).

4.14. Animal experiment

An intrabone injection model of bone metastasis was used to confirm the *in vitro* results. All procedures were performed in compliance with the Xi'an Jiaotong University of Animal Care and Use Committee. Six-week-old male severe combined immunodeficiency disease (SCID) mice were housed in a facility with constant humidity and temperature and a 12-h light–dark cycle. After the animals were anesthetized with i.m. injections of 100 mg ketamine/10 mg xylazine/kg body weight, a 26-gauge needle was inserted into the proximal end of the tibia and 100 μL of cell preparation containing 1×10^6 control or DDR2-depleted PC-3 cells was injected. The same volume of PBS was injected as negative control. Animals were monitored daily for signs of tumor burden. After 3 weeks, radiographs of the bones were obtained (35 kV, 15 s, 20.7 mA/s, small focal setting).

4.15. Statistical analysis

Each experiment was repeated at least three times, unless indicated otherwise. The results obtained from a typical experiment were expressed as the mean ± standard deviation. Statistical analysis was performed using GraphPad Prism 4. Significant differences were determined using students *t* test, p value less than 0.05 was considered significant.

Conflict of interest

The authors declare that they have no competing interests.

Acknowledgments

This work is supported by the National Natural Science Foundation of China (No. 81300716), the Specialized Research Fund for the Doctoral Program of Higher Education (No. 20120201120089) and the Scientific Research Fund of Shaanxi Provincial Department of Health (No. 2012D59).

Appendix A. Supplementary data

Supplementary data to this article can be found online at http://dx.doi.org/10.1016/j.bbadis.2014.04.018.

References

[1] A. Jemal, F. Bray, M.M. Center, J. Ferlay, E. Ward, D. Forman, Global cancer statistics, CA Cancer J. Clin. 61 (2) (Mar-Apr 2011) 69–90.
[2] P.D. Baade, D.R. Youlden, L.J. Krnjacki, International epidemiology of prostate cancer: geographical distribution and secular trends, Mol. Nutr. Food Res. 53 (2) (Feb 2009) 171–184.
[3] A. Jemal, R. Siegel, E. Ward, Y. Hao, J. Xu, T. Murray, M.J. Thun, Cancer statistics, CA Cancer J. Clin. 58 (2) (Mar-Apr 2008) 71–96.
[4] A. Lorch, Metastatic prostate cancer: new insights and developments, Dtsch. Med. Wochenschr. 138 (14) (Apr 2013) 703–706.
[5] G.D. Roodman, Genes associate with abnormal bone cell activity in bone metastasis, Cancer Metastasis Rev. 31 (3–4) (Dec 2012) 569–578.
[6] S. Casimiro, T.A. Guise, J. Chirgwin, The critical role of the bone microenvironment in cancer metastases, Mol. Cell. Endocrinol. 310 (1–2) (Oct 30 2009) 71–81.
[7] T. Yoneda, Mechanism and strategy for treatment of cancer metastasis to bone, Gan To Kagaku Ryoho 38 (6) (Jun 2011) 877–884.
[8] P. Juárez, T.A. Guise, TGF-β in cancer and bone: implications for treatment of bone metastases, Bone 48 (1) (Jan 2011) 23–29.
[9] J.T. Buijs, P. Juárez, T.A. Guise, Therapeutic strategies to target TGF-β in the treatment of bone metastases, Curr. Pharm. Biotechnol. 12 (12) (Dec 2011) 2121–2137.
[10] R. Faccio, Immune regulation of the tumor/bone vicious cycle, Ann. N. Y. Acad. Sci. 1237 (Nov 2011) 71–78.
[11] F.N. Soki, S.I. Park, L.K. McCauley, The multifaceted actions of PTHrP in skeletal metastasis, Future Oncol. 8 (7) (Jul 2012) 803–817.
[12] S. Isowa, T. Shimo, S. Ibaragi, N. Kurio, T. Okui, K. Matsubara, N.M. Hassan, K. Kishimoto, A. Sasaki, PTHrP regulates angiogenesis and bone resorption via VEGF expression, Anticancer Res. 30 (7) (Jul 2010) 2755–2767.
[13] J. Liao, X. Li, A.J. Koh, J.E. Berry, N. Thudi, T.J. Rosol, K.J. Pienta, L.K. McCauley, Tumor expressed PTHrP facilitates prostate cancer-induced osteoblastic lesions, Int. J. Cancer 123 (10) (Nov 15 2008) 2267–2278.
[14] I.W. Mak, R.W. Cowan, R.E. Turcotte, G. Singh, M. Ghert, PTHrP induces autocrine/paracrine proliferation of bone tumor cells through inhibition of apoptosis, PLoS One 6 (5) (2011) e19975.
[15] R. Kremer, J. Li, A. Camirand, A.C. Karaplis, Parathyroid hormone related protein (PTHrP) in tumor progression, Adv. Exp. Med. Biol. 720 (2011) 145–160.
[16] N. Rucci, A. Teti, Osteomimicry: how tumor cells try to deceive the bone, Front. Biosci. (Schol. Ed.) 2 (Jun 1 2010) 907–915.
[17] J. Pratap, J.B. Lian, A. Javed, G.L. Barnes, A.J. van Wijnen, J.L. Stein, G.S. Stein, Regulatory roles of Runx2 in metastatic tumor and cancer cell interactions with bone, Cancer Metastasis Rev. 25 (4) (Dec 2006) 589–600.
[18] J. Akech, J.J. Wixted, K. Bedard, M. van der Deen, S. Hussain, T.A. Guise, A.J. van Wijnen, J.L. Stein, L.R. Languino, D.C. Altieri, J. Pratap, E. Keller, G.S. Stein, J.B. Lian, Runx2 association with progression of prostate cancer in patients: mechanisms mediating bone osteolysis and osteoblastic metastatic lesions, Oncogene 29 (6) (Feb 11 2010) 811–821.
[19] J. Pratap, J.B. Lian, G.S. Stein, Metastatic bone disease: role of transcription factors and future targets, Bone 48 (1) (Jan 2011) 30–36.
[20] S.K. Baniwal, O. Khalid, Y. Gabet, R.R. Shah, D.J. Purcell, D. Mav, A.E. Kohn-Gabet, Y. Shi, G.A. Coetzee, B. Frenkel, Runx2 transcriptome of prostate cancer cells: insights into invasiveness and bone metastasis, Mol. Cancer 9 (Sep 23 2010) 258.

[21] J. Pratap, J.J. Wixted, T. Gaur, S.K. Zaidi, J. Dobson, K.D. Gokul, S. Hussain, A.J. van Wijnen, J.L. Stein, G.S. Stein, J.B. Lian, Runx2 transcriptional activation of Indian Hedgehog and a downstream bone metastatic pathway in breast cancer cells, Cancer Res. 68 (19) (Oct 1 2008) 7795–7802.
[22] A. Javed, G.L. Barnes, J. Pratap, T. Antkowiak, L.C. Gerstenfeld, A.J. van Wijnen, J.L. Stein, J.B. Lian, G.S. Stein, Impaired intranuclear trafficking of Runx2 (AML3/CBFA1) transcription factors in breast cancer cells inhibits osteolysis *in vivo*, Proc. Natl. Acad. Sci. U. S. A. 102 (5) (Feb 1 2005) 1454–1459.
[23] A. Shrivastava, C. Radziejewski, E. Campbell, L. Kovac, M. McGlynn, T.E. Ryan, S. Davis, M.P. Goldfarb, D.J. Glass, G. Lemke, G.D. Yancopoulos, An orphan receptor tyrosine kinase family whose members serve as nonintegrin collagen receptors, Mol. Cell 1 (1) (Dec 1997) 25–34.
[24] W. Vogel, G.D. Gish, F. Alves, T. Pawson, The discoidin domain receptor tyrosine kinases are activated by collagen, Mol. Cell 1 (1) (Dec 1997) 13–23.
[25] L.A. Vonk, B.Z. Doulabi, C. Huang, M.N. Helder, V. Everts, R.A. Bank, Collagen-induced expression of collagenase-3 by primary chondrocytes is mediated by integrin α1 and discoidin domain receptor 2: a protein kinase C-dependent pathway, Rheumatology (Oxford) 50 (3) (Mar 2011) 463–472.
[26] L. Sivakumar, G. Agarwal, The influence of discoidin domain receptor 2 on the persistence length of collagen type I fibers, Biomaterials 31 (18) (Jun 2010) 4802–4808.
[27] J. Su, J. Yu, T. Ren, W. Zhang, Y. Zhang, X. Liu, T. Sun, H. Lu, K. Miyazawa, L. Yao, Discoidin domain receptor 2 is associated with the increased expression of matrix metalloproteinase-13 in synovial fibroblasts of rheumatoid arthritis, Mol. Cell. Biochem. 330 (1–2) (Oct 2009) 141–152.
[28] I. Kawai, T. Hisaki, K. Sugiura, K. Naito, K. Kano, Discoidin domain receptor 2 (DDR2) regulates proliferation of endochondral cells in mice, Biochem. Biophys. Res. Commun. 427 (3) (Oct 26 2012) 611–617.
[29] H. Xu, D. Bihan, F. Chang, P.H. Huang, R.W. Farndale, B. Leitinger, Discoidin domain receptors promote α1β1- and α2β1-integrin mediated cell adhesion to collagen by enhancing integrin activation, PLoS One 7 (12) (2012) e52209.
[30] D. Kim, E. You, N.Y. Min, K.H. Lee, H.K. Kim, S. Rhee, Discoidin domain receptor 2 regulates the adhesion of fibroblasts to 3D collagen matrices, Int. J. Mol. Med. 31 (5) (May 2013) 1113–1118.
[31] P.A. Ruiz, G. Jarai, Discoidin domain receptors regulate the migration of primary human lung fibroblasts through collagen matrices, Fibrogenesis Tissue Repair 5 (1) (Feb 15 2012) 3.
[32] M.L. Herrera-Herrera, R. Quezada-Calvillo, DDR2 plays a role in fibroblast migration independent of adhesion ligand and collagen activated DDR2 tyrosine kinase, Biochem. Biophys. Res. Commun. 429 (1–2) (Dec 7 2012) 39–44.
[33] Yan Zhang, Su. Jin, Yu. Jiangtian, Bu. Xin, Tingting Ren, Libo Yao, An essential role of discoidin domain receptor 2 (DDR2) in osteoblast differentiation and chondrocyte maturation via modulation of Runx2 activation, J. Bone Miner. Res. 26 (3) (Mar 2011) 604–617.
[34] K.L. Lin, C.H. Chou, S.C. Hsieh, S.Y. Hwa, M.T. Lee, F.F. Wang, Transcriptional upregulation of DDR2 by ATF4 facilitates osteoblastic differentiation through p38 MAPK-mediated Runx2 activation, J. Bone Miner. Res. 25 (11) (Nov 2010) 2489–2503.
[35] I. Badiola, P. Villacé, I. Basaldua, E. Olaso, Downregulation of discoidin domain receptor 2 in A375 human melanoma cells reduces its experimental liver metastasis ability, Oncol. Rep. 26 (4) (Oct 2011) 971–978.
[36] N. Beauchemin, The colorectal tumor microenvironment: the next decade, Cancer Microenviron. 4 (2) (Aug 2011) 181–185.
[37] H.H. Chua, T.H. Yeh, Y.P. Wang, Y.T. Huang, T.S. Sheen, Y.C. Lo, Y.C. Chou, C.H. Tsai, Upregulation of discoidin domain receptor 2 in nasopharyngeal carcinoma, Head Neck 30 (4) (Apr 2008) 427–436.
[38] R. Rodrigues, L. Roque, C. Espadinha, A. Pinto, R. Domingues, J. Dinis, A. Catarino, T. Pereira, V. Leite, Comparative genomic hybridization, BRAF, RAS, RET, and oligo-array analysis in aneuploid papillary thyroid carcinomas, Oncol. Rep. 18 (4) (Oct 2007) 917–926.
[39] K. Zhang, C.A. Corsa, S.M. Ponik, J.L. Prior, D. Piwnica-Worms, K.W. Eliceiri, P.J. Keely, G.D. Longmore, The collagen receptor discoidin domain receptor 2 stabilizes SNAIL1 to facilitate breast cancer metastasis, Nat. Cell Biol. 15 (6) (Jun 2013) 677–687.
[40] T. Ren, J. Zhang, J. Zhang, X. Liu, L. Yao, Increased expression of discoidin domain receptor 2 (DDR2): a novel independent prognostic marker of worse outcome in breast cancer patients, Med. Oncol. 30 (1) (Mar 2013) 397.
[41] Vesna Evtimova, Robert Zeillinger, Ulrich H. Weidle, Identification of genes associated with the invasive status of human mammary carcinoma cell lines by transcriptional profiling, Tumor Biol. 24 (2003) 189–198.
[42] L.A. Walsh, A. Nawshad, D. Medici, Discoidin domain receptor 2 is a critical regulator of epithelial–mesenchymal transition, Matrix Biol. 30 (4) (May 2011) 243–247.
[43] C. Ge, G. Xiao, D. Jiang, et al., Identification and functional characterization of ERK/MAPK phosphorylation sites in the Runx2 transcription factor, J. Biol. Chem. 284 (2009) 32533–32543.
[44] I. Badiola, E. Olaso, O. Crende, S.L. Friedman, F. Vidal-Vanaclocha, Discoidin domain receptor 2 deficiency predisposes hepatic tissue to colon carcinoma metastasis, Gut 61 (10) (Oct 2012) 1465–1472.
[45] P.L. Kuo, S.H. Liao, J.Y. Hung, M.S. Huang, Y.L. Hsu, MicroRNA-33a functions as a bone metastasis suppressor in lung cancer by targeting parathyroid hormone related protein, Biochim Biophys Acta 1830 (6) (2013 Jun) 3756–3766